

TOMOGRAPHIC IMAGING OF THE IONOSPHERE DENSITY

Xiaojian Xu*

Washington University in St. Louis
St. Louis, MO 63130
xiaojianxu@wustl.edu

Hassan Mansour, Petros T. Boufounos, Philip V. Orlik

Mitsubishi Electric Research Laboratories
Cambridge, MA 02139
{mansour, petrosb, porlik}@merl.com

ABSTRACT

In this paper, we develop a three dimensional tomographic imaging framework to estimate the ionospheric electron density using ground-based total electron content (TEC) measurements from GPS receivers. Contrary to previous methods, we incorporate into the tomographic measurements the TEC readings observed from low-angle satellites that fall outside of the target ionospheric domain. We utilize simulation-based NeQuick models to discount the proportion of the TEC measurements that originate outside of the target domain. We also construct an efficient forward modeling operator that allows for significant scaling of the number of TEC measurements. Together, with the inclusion of improved regularization functions, we demonstrate that our framework delivers superior reconstruction of simulated ionospheric electron density maps. We also demonstrate the applicability of our approach on real TEC measurements.

Index Terms— Ionosphere Mapping, GPS, Tomographic Imaging, Total Electron Content

1. INTRODUCTION

Electrons are distributed around earth from altitude around 80km to 20000km, acting as a transportation medium to the global position system (GPS) satellite signals. Referred as ionosphere, this region has practical importance as it influences radio propagation to receivers on the Earth. Therefore the inference of ionosphere density distribution has long been one of the focus in the ionospheric study. After the proposal of the ionospheric tomography technique using the TEC along the LOS from naval navigational satellite system (NNSS) to the ground-based receivers in [1] [2], such computerized ionospheric tomography (CIT) technology has been developed in many related researches. A general idea of CIT is to use the 2-D ground based measurements TEC, which is a accumulated result of the electron density distribution along a LOS to infer the unknown 3-D ionosphere density distribution. The relationship between TEC and the ionosphere

density distribution are

$$\text{TEC}_i = \int_{rec}^{sat} N_e(\rho) d\rho, \quad (1)$$

where i indicates the i -th LOS, and $N_e(\rho)$ denotes the electron density along this LOS connecting the receiver rec and the satellite sat . By dividing the three-dimensional space into small grids and assuming homogeneity of the density inside each grid, we could discrete this model as

$$\text{TEC}_i = \sum_{k=1}^n a_{ik} x_k, \quad (2)$$

where n is the total number of grids, a_{ik} denotes the length of path i in grid k , and x_k denotes the electron density in grid k . Note that in this case, when the LOS i does not pass through grid k , a_{ik} is set to zero. Apparently this linear model could be represented in the following matrix form:

$$\mathbf{y} = \mathbf{Ax}, \quad (3)$$

where $\mathbf{y} \in \mathbb{R}^m$ denotes the 2-D ground based TEC measurements, $\mathbf{A} \in \mathbb{R}^{m \times n}$ denotes the linear forward model and $\mathbf{x} \in \mathbb{R}^n$ is the vectored ionosphere density distribution that we want to infer. With the TEC measurements provided by the GPS message files transferred between GPS satellites and receivers, the inference of electron density distribution could be formulated as an inverse problem. Figure 1 shows a simple illustration of this 3-D model.

2. PRIOR WORK

Although dense ground-based GPS receivers are deployed, due to the fact that only a few of high elevation LOS ray passes through the region of interest (ROI) thus few TEC measurements information, such a ill-posed inverse problem is still difficult to straightforwardly solve. Some CIT methods requires an initial guess value from the ionospheric model[3] [4]. Work in [5] proposed a least square method without model-based initialization. But the constrain parameters in the paper is empirical and model-based. The work in [6]

*X. Xu performed this work during an internship at MERL.

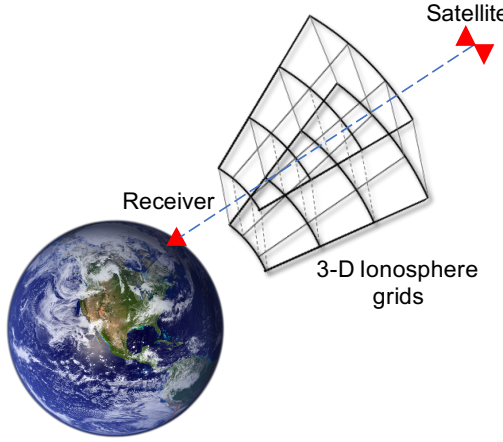


Fig. 1. A simple illustration of 3-D Ionosphere tomography model with one LOS.

follow the similar idea with model-free diffusion kernel constrain. [7] uses the Neural Network to reconstruct 3-D electron density using GPS-TEC and ionosonde data, giving a effective estimation of vertical profile. However, none of those methods were able to take advantage of the low elevation LOS paths, which are in fact the majority of the measurements. Therefore, in this study, we would develop a methodology using all elevation TEC measurements, including low elevation ones that only partially intersects with our ROI. We show with the experiments that such comprehensive TEC mesurements will greatly improve our reconstruction accuracy.

3. MAIN METHOD

In this section, we introduce how we compute our TEC measurements \mathbf{y} and forward model \mathbf{A} from the raw GPS data, and then we give our reconstruction method.

3.1. Computation of measurements \mathbf{y} from GPS data

There are 28 GPS satellites currently orbiting the Earth at a height of 20200 km broadcasting information on two frequency carrier signals via GPS message files. These two radio signals are delayed by different amount and based on these delays, two known ways to compute TEC are derived [8], where the first one is based on the pesudo-ranges P_1 and P_2 (referred as TEC_{pr}) and the second one is based on carrier phase L_1 and L_2 (referred as TEC_{cp}):

$$\text{TEC}_{pr} = \frac{2}{k} \frac{f_1^2 f_2^2}{f_1^2 - f_2^2} (P_2 - P_1), \quad (4)$$

$$\text{TEC}_{cp} = \frac{2c}{k} \frac{f_1^2 f_2^2}{f_1^2 - f_2^2} (L_1/f_1 - L_2/f_2). \quad (5)$$

Note here $k = 80.62(m^3/s^2)$ is the ionosphere refraction, c is the speed of light, and $f_1 = 1.57542\text{GHz}$, $f_2 = 1.2276\text{GHz}$ are two frequencies satellites transmit on. Though these two types of TEC provide estimations of the TEC, none of them are accurate. TEC_{pr} is very noisy, while TEC_{cp} is less noisy but it is a relative value with cycle spin issues. Therefore, many work has been done on the refining of such raw TEC estimation [9, 10, 11, 12]. In this study, we follow the method introduced in [13] and compute the GPS-TEC by combining TEC_{cp} and TEC_{pr} together. A series of refining operations were also done to remove the ambiguity and correct the cycle slips, estimate the instrument biases, smooth the vertical TEC (vTEC). We leave the details to [13] due to the page limitation.

The GPS-TEC measurement we compute above is a accumulation of ionosphere density along the whole LOS path. Note that one low elevation LOS may just partially pass through the 3-D ROI, meaning that the measurement \mathbf{y} accounts for the intersection part of this LOS and the 3-D tomography should be smaller than such GPS-TEC. We assume that the GPS-TEC inside the ROI along a LOS is proportional to the TEC inside the ROI of a reference model, NeQuick [14]. NeQuick is a known model that predicts monthly mean electron density from analytical profiles. Therefore we use the NeQuick-TEC to compensate for the mismatch of \mathbf{y} and GPS-TEC, which allows us to use such low angel GPS-TEC measurements in our reconstruction. We refer such TEC as full measurements and its counterpart high elevation ones as partial measurements in the later section. We will see in the experiment section that such a full measurements is very beneficial to the reconstruction. Note that we could also set a tuning matrix to adjust the weight of such low angel measurements, we simply ignore such tricks in this paper due to the page limitation and simplicity.

3.2. Construction of forward model \mathbf{A} with low elevation measurements

As we introduced at the beginning, \mathbf{A} is a linear model where each row is a collection of distances a LOS connecting a pair of receiver and satellite passing through the 3-D ionosphere volume, and each element in a row of \mathbf{A} represents the distance a satellite-receiver ray travels inside a grid [15]. To compute these distances is to compute the coordinate of two intersection points of the ray and the grid. Though the intersection point could be located at any two different plane of the grid, there are only three types of intersection points under the assumption that the Earth is a sphere. The first type intersection points are in altitude sphere. The second type of intersection points are in latitude cone. The third type of intersection points are in longitude plane. Therefore, to compute the forward model is to compute the intersections of a ray with a sphere, a cone and a plane and the distance between these intersections. By assuming the the Earth is a sphere,

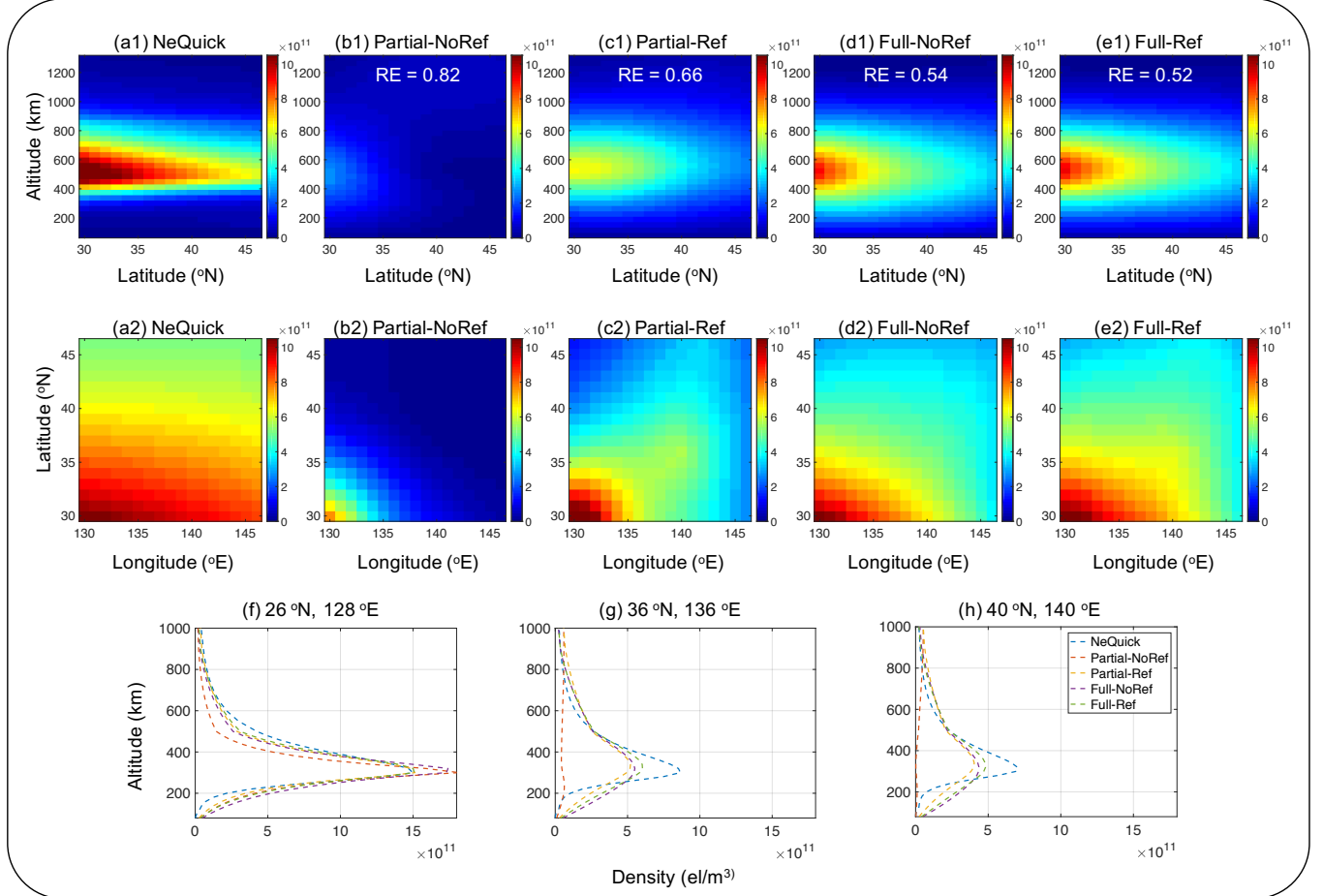


Fig. 2. Comparison of four simulation-based experiments. The first row (a1)-(e1) show the altitude-latitide profile with altitude fixed at 360km, the second row (a2)-(e2) shows the latitude-longitude plot with longitude fixed as 135°E and the third row (f)-(h)shows the vertical profile at [128°E, 26°N], [136°E, 36°N] and [140°E, 40°N].

these could be easily solved as a ray tracing problem using the location information from GPS data.

3.3. Reconstruction method

Based on the model brought up in the previous work [6], we propose our least square method with ionosonde references data constrains:

$$\begin{aligned} \hat{\mathbf{x}} = \arg \min_{\mathbf{x} \in \mathbb{R}^n} & \| \mathbf{y} - \mathbf{Ax} \|_2^2 + \lambda \| \mathbf{Wx} \|_2^2 + \gamma \sum_{q=1}^h \| \mathbf{R}_q \mathbf{x} - x_q \|_2^2 \\ \text{s.t. } & \mathbf{x} \geq 0, \end{aligned} \quad (6)$$

where \mathbf{y} is the TEC measurements computed by method in Section 3.1 and \mathbf{A} is our forward model computed by the ray tracing method described in Section ???. $\mathbf{W} \in \mathbb{R}^{n \times n}$ is a constraint matrix where in the i -th row, six neighbors of the grid x_i are assigned to 1, x_i is assigned to 6 and others are

to 0. Therefore \mathbf{W} works as a 3×3 diffusion kernel that denotes the coupling of the ionosphere density in grid i with the ionosphere density in its six neighbors:

$$\mathbf{Wx} = \sum_{i=1}^N \sum_{k=1}^6 C_{ik} (x_i - x_{ik}). \quad (7)$$

Note here $C_{ik} \geq 0$ is a constrain parameter that indicate the weighting of these six neighbors. Inspired by the idea in [6] that the constrain should be loose in region where the density changes fast and tight in region changes slow along the altitude, we define the constraint parameters C_i as a function of the latitude, longitude, and altitude based on the empirical electron density model NeQuick:

$$C_i = \frac{(1 - vTEC_{NeQuick}^i / (vTEC_{NeQuick}^{max} + R))^{1.2}}{10}. \quad (8)$$

Here $vTEC_{NeQuick}^i$ denotes a group of NeQuick vertical TEC at a given latitude and longitude , $vTEC_{NeQuick}^{max}$ is the maxi-

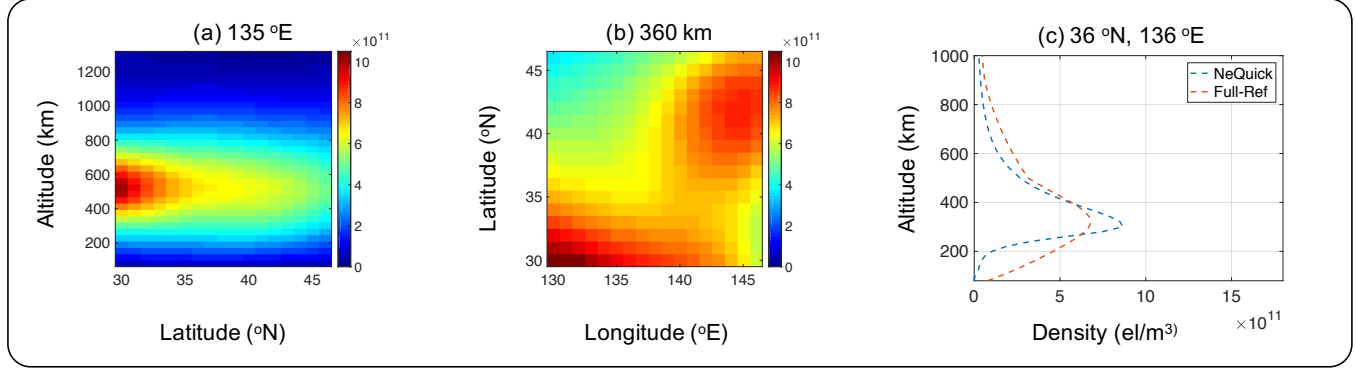


Fig. 3. 2-D visualization of 3-D reconstruction results on the GPS-based measurements. (a), (b) and (c) shows the altitude-latitude profile, latitude-longitude profile and vertical profile of TEC separately.

mum density distribution along this vTEC, and $R = 1.0 \times 10^{11} (\text{el}/\text{m}^3)$ is an adjustment constant.

The last term in (6) is our reference constrain term. $\mathbf{R}_q \in \mathbb{R}^n$ is a binary selection mask that extract the vertical TEC at some given positions, h is the total number of those reference points at given positions. Therefore, the last term constrains the alignment of the reconstruction and the real ionosphere references. $\lambda \geq 0$ and $\gamma \geq 0$ are the regularization weighting parameters. In fact if we set $\lambda = 0$, this is an similar frame work proposed in [6]. We refer $\lambda = 0$ case as ‘‘NoRef’’ and its counterpart as ‘‘Ref’’ in later section. We will later show that by introducing our reference constrain model, we are able to have a better reconstruction performance.

4. MAIN RESULTS

4.1. Experiment settings

In the following experiments, we focus on the reconstruction of 3-D ionosphere density model in the region of Japan at 10:00 UT on May 23, 2012. We chose 195 ground GPS receivers and select the vertical TEC references x_q as the value at $[141.75^\circ E, 45.16^\circ N]$, $[139.49^\circ E, 35.71^\circ N]$, $[130.62^\circ E, 31.20^\circ N]$ and $[128.15^\circ E, 26.68^\circ N]$, since those are four real ionosonde stations in Japan that could measure the vertical TECs. In altitude dimension, the vertical range of tomography is set from 80 to 20000km. The vertical resolutions are 20km within 80 – 500km, 50km within 500 – 900km, 100km within 900 – 2000km range, 1000km within 2000 – 5000km, and 5000km within 5000 – 20000km. The horizontal resolution is set to 1° , in which the latitudinal range is $22^\circ N$ to $56^\circ N$ and the longitudinal range is $118^\circ E$ to $178^\circ E$. To measure the accuracy of our reconstruction, we use the following relative error (RE):

$$RE = \|\hat{\mathbf{x}} - \mathbf{x}^*\|_2 / \|\mathbf{x}^*\|_2, \quad (9)$$

where $\hat{\mathbf{x}}$ is the reconstruction results and \mathbf{x}^* is its ground truth.

4.2. Experiment results

To demonstrate the feasibility of our reconstruction method, we first conduct a simulation-based experiment where we use NeQuick model to generate the ground truth \mathbf{x}^* and then use the geometry between GPS satellites and GPS receivers to generate the forward model **A**. We synthesis the measurements TEC by multiplying **A** and \mathbf{x}^* together. To show the benefits of using full elevation measurements and our reference points, we do four experiments: using partial measurements with out reference constrain(referred as Partial-NoRef), using partial measurements with reference constrain(referred as Partial-Ref), using full measurements without reference constrain(referred as Full-Ref), using full measurements with reference constrain(referred as Full-Ref). Figure2 shows the reconstruction of our simulation-based experiment. We could see that when the full measurements are used, we could greatly reduce the reconstruction error and get reasonable reconstruction results.

We also perform the GPS-based experiment where we use the true measurements from GPS-TEC. Figure 3 shows the reconstruction results. Note that though we don’t have ground truth data in this case, comparing with NeQuick model, we could see that our method are able to generate a reasonable results.

5. CONCLUSION

In this study we managed to use all elevation GPS-TEC to reconstruct 3-D ionosphere density. We show with simulation and real data experiments that such technology could greatly improve the reconstruction performance. Further study could investigate in developing a more accurate discount methodology of the out-grid TEC.

6. REFERENCES

- [1] JR Austen, SJ Franke, CH Liu, and KC Yeh, “Application of computerized tomography techniques to ionospheric research,” in *international beacon satellite symposium on radio beacon contribution to the study of ionization and dynamics of the ionosphere and to corrections to geodesy and technical workshop*, 1986, pp. 25–35.
- [2] Jeffrey R Austen, Steven J Franke, and CH Liu, “Ionospheric imaging using computerized tomography,” *Radio Science*, vol. 23, no. 3, pp. 299–307, 1988.
- [3] TD Raymund, “Comparison of several ionospheric tomography algorithms,” *Ann. Geophys.*, vol. 13, pp. 1254–1262, 1995.
- [4] Dieter Bilitza and Bodo W Reinisch, “International reference ionosphere 2007: Improvements and new parameters,” *Advances in space research*, vol. 42, no. 4, pp. 599–609, 2008.
- [5] Gopi K Seemala, Mamoru Yamamoto, Akinori Saito, and Chia-Hung Chen, “Three-dimensional gps ionospheric tomography over japan using constrained least squares,” *Journal of Geophysical Research: Space Physics*, vol. 119, no. 4, pp. 3044–3052, 2014.
- [6] Chia-Hung Chen, A Saito, Chien-Hung Lin, M Yamamoto, S Suzuki, and Gopi K Seemala, “Medium-scale traveling ionospheric disturbances by three-dimensional ionospheric gps tomography,” *Earth, Planets and Space*, vol. 68, no. 1, pp. 32, 2016.
- [7] XF Ma, T Maruyama, G Ma, and T Takeda, “Three-dimensional ionospheric tomography using observation data of gps ground receivers and ionosonde by neural network,” *Journal of Geophysical Research: Space Physics*, vol. 110, no. A5, 2005.
- [8] Geoffrey Blewitt, “An automatic editing algorithm for gps data,” *Geophysical research letters*, vol. 17, no. 3, pp. 199–202, 1990.
- [9] Y Otsuka, T Ogawa, A Saito, T Tsugawa, S Fukao, and S Miyazaki, “A new technique for mapping of total electron content using gps network in japan,” *Earth, planets and space*, vol. 54, no. 1, pp. 63–70, 2002.
- [10] Lo Ciraolo, F Azpilicueta, C Brunini, A Meza, and SM Radicella, “Calibration errors on experimental slant total electron content (tec) determined with gps,” *Journal of Geodesy*, vol. 81, no. 2, pp. 111–120, 2007.
- [11] F Arikan, H Nayir, U Sezen, and O Arikan, “Estimation of single station interfrequency receiver bias using gps- tec,” *Radio Science*, vol. 43, no. 4, 2008.
- [12] T Tsugawa, A Saito, and Y Otsuka, “A statistical study of large-scale traveling ionospheric disturbances using the gps network in japan,” *Journal of Geophysical Research: Space Physics*, vol. 109, no. A6, 2004.
- [13] G Ma and T Maruyama, “Derivation of tec and estimation of instrumental biases from geonet in japan,” in *Annales Geophysicae*, 2003, vol. 21, pp. 2083–2093.
- [14] SM Radicella and R Leitinger, “The evolution of the dgr approach to model electron density profiles,” *Advances in Space Research*, vol. 27, no. 1, pp. 35–40, 2001.
- [15] Fabricio dos Santos Prol and Paulo de Oliveira Camargo, “Review of tomographic reconstruction methods of the ionosphere using gnss,” *Revista Brasileira de Geofísica*, vol. 33, no. 3, pp. 445–459, 2015.